



Narrowband Elliptic Bandpass Filter Using Dual-Mode Microstrip Square Loop Resonator for WiMax Application

Babak Kazemi Esfeh

Department of Computer and Communication Systems Engineering

Faculty of Engineering, Universiti Putra Malaysia

43400 Serdang, Malaysia

Tel: 60-3-8946-4352, Fax: 60-3-8656-7127 E-mail: kiaertebat2004@yahoo.com

Alyani Ismail

Department of Computer and Communication Systems Engineering

Faculty of Engineering, Universiti Putra Malaysia

43400 Serdang, Malaysia

Tel: 60-3-8946-4352, Fax: 60-3-8656-7127 E-mail: alyani@eng.upm.edu.my

Raja Syamsul Azmir Raja Abdullah

Department of Computer and Communication Systems Engineering

Faculty of Engineering, Universiti Putra Malaysia

43400 Serdang, Malaysia

Tel: 60-3-8946-4352, Fax: 60-3-8656-7127 E-mail: rsa@eng.upm.edu.my

Abstract

In this paper, a narrowband bandpass filter using dual-mode microstrip square loop resonator is proposed. This structure has a 5.1% fractional bandwidth at 2.3GHz. By using some simple techniques, the optimum results will be achieved. The dual-mode resonator will be produced by adding a square patch inside the loop resonator. The simulation and measurement results are also presented. The filter is fabricated on RT/Duroid 6010 substrate having a relative dielectric constant of 10.2 and 0.635 mm thickness. The final dimension is measured at 19.65 mm × 19.65 mm. The minimum measured insertion loss is 1.68 dB and return loss obtained is better than -20 dB, where experimental results and simulated values are in good agreement.

Keywords: Dual-mode bandpass filter

1. Introduction

In comparison with waveguide filters, microstrip filters are smaller, but in some applications, there are needs to have smaller microstrip filters. Nowadays satellite and mobile communication systems are such applications that size reduction is of primary importance (Pozar, 2005). Of course, in addition to size reduction many other parameters in filter designing should be considered, such as low insertion loss, high return loss and high rejection band, where these are the characteristics of a good filter. Furthermore, lightweight and cost-effective filters are always desired. Although miniaturization of microstrip filters can be achieved by using high dielectric constant substrates, reduction in size with changing the filters geometry is more desirable, because high dielectric permittivity will often introduce more surface waves and losses. One useful method to achieve a compact size in filter designing is to have its different parts bended. This could be an optimum solution to get more compact in sizes especially for filters with stubs and long straight transmission lines. Ultra-wideband filters reported in (Razalli, 2008) and wideband filter reported in (El-Shaarawy, 2008) are among the structures making use of method of bending the lines. On the other hand, filters using dual-mode microstrip ring or square loop resonator are other techniques of minimizing microstrip filter structures (Hong, 1995).

The main advantage of using these types of resonators is that in dual-mode resonator, each resonator acts as a double tuned resonant circuit and therefore, an n -degree filter can be achieved in more compact configurations and less complicated due to the halved number of resonators (Hong, 2001). Various designs of dual-band filters are widely used as necessary filters in wireless industry and communication systems. A major portion of these designs utilizes dual-mode resonators. Among dual-mode resonators, those using patch, attract more interest and are used in both single band and dual-band filters (Chen, 2007). In this paper, a square form of dual-mode microstrip loop resonator with additional square patch perturbation technique for WiMax application is proposed with the aim to provide simple configuration with compactness in nature.

2. Dual-Mode Microstrip Resonators

A microstrip dual-mode resonator in any shape, having symmetry in two dimension (2-D), can be described by Wheeler’s cavity model. In this model, the top and bottom of the cavity are complete electric walls and the other sides are perfect magnetic walls. Therefore, three parameters, namely E_z , H_x , and H_y represent the Electro-Magnetic (EM) fields inside the cavity in terms of TM_{mn0}^z modes. Different modes introduce limitless resonant frequencies, which can be expressed by (Hong, 2001)

$$f_{mn0} = \frac{c}{2\pi\sqrt{\mu\epsilon_{eff}}} \sqrt{\left(\frac{m\pi}{a}\right)^2 + \left(\frac{n\pi}{a}\right)^2} \tag{1}$$

Where μ and ϵ_{eff} are permeability and effective dielectric constant of the used substrate respectively, and a is the effective width of the cavity.

By substituting proper values for m and n , equal frequencies can be obtained. For instance, $f_{100} = f_{010}$ and $f_{110} = f_{101}$. These modes are degenerate modes that have the same resonant frequency with orthogonal field distributions. Therefore, they have no coupling and no effect to each other. When some perturbations are added to the symmetry of the structure, the field distributions of them will be no longer orthogonal and couple to each other. In this condition, two coupled degenerate modes act like two coupled resonators and a two-pole dual-mode microstrip filter can be achieved. This is the simplest dual-mode bandpass filter using a single dual-mode resonator (Hong, 2001, Wolff, 1971 and Curtis, 1991). Figure 1 illustrates the equivalent lumped elements of coupled degenerate modes. The field theory for the ring resonator has been presented by Wolff and Knoppik (Wolff, 1971). In this theory only the frequency modes of the annular ring resonator has been derived. For closed loop resonators in shape of n -side polygon, because of their complex boundary condition, it is difficult to use magnetic-wall model to obtain the frequency modes. Thus, the best way is that they be considered as a special case of an annular ring resonator, though it is not a precise approximation (Chang, 2004). It is obvious that as n increases, better approximation can be achieved.

3. Design of Dual-Mode Microstrip Square Loop Resonator

The design of the proposed dual-mode microstrip resonator has been conducted for WiMax operating frequency of 2.3GHz and fabricated on a RT/Duroid substrate having 0.635mm thickness and a relative dielectric constant of 10.2. The layout of the resonator is depicted in Figure 2(a). It is shown in Figure 2(a) that the resonator is excited by using gap-coupling method where input port, *port 1* and output port, *Port 2* are spaced with a gap, G symmetrically on each side.

The resonator (basic part of our filter), is designed to resonate at 2.3GHz. Equations (2) and (3) are used to synthesize W/h (the conductor width and substrate thickness of microstrip) in terms of characteristic impedance (Z_0) and substrate dielectric permittivity (ϵ_r) (Hong, 2001),

$$\frac{W}{h} = \frac{8e^A}{e^{2A}-2} \quad \left(\frac{W}{h} \leq 2\right) \tag{2}$$

$$A = \frac{Z_0}{60} \sqrt{\frac{\epsilon_r-1}{2} + \frac{\epsilon_r-1}{\epsilon_r+1} \left(0.23 + \frac{0.11}{\epsilon_r}\right)} \tag{3}$$

The circumference of the ring resonator ℓ_r is calculated according to the following expression (chang, 2004):

$$\ell_r = n\lambda_g \tag{4}$$

Where n is the mode number and λ_g is the guided wavelength. The design is done for the first mode. The trace width (W) of 0.576 mm will produce a 50Ω characteristic impedance line and each side of the square loop resonator is $a = 12.2$ mm (one quarter of wavelength). The structure shown in Figure 2(a) is simulated using EM simulator software (EM, 2006) and simulated insertion loss and return loss for different values of feedlines gap, G are shown in Figure 2(b).

As can be seen in the simulation results, coupling gaps between the resonator and feedlines, G affect the resonant frequency. With smaller gap size, the insertion loss is lower and the resonant frequency is more affected, and bigger gap size causes higher insertion loss and lower affection on the resonant frequency. Therefore, by adjusting the gap sizes the

desired values for insertion loss and resonant frequency can be achieved.

4. Design of Narrowband Elliptic Bandpass Filter Using Dual-Mode Microstrip Square Loop Resonator

The structure of the single mode resonator shown in Figure 2(a) has been transformed into a dual-mode resonator shown in Figure 3 to create a narrowband bandpass filter. The feedlines positions excite two degenerate modes, T_{100}^z , and T_{010}^z . When $d = 0$, there is no perturbation and just a single mode is excited. In the T_{100}^z mode, the *port 1* is excited and we have two zeros located in the middle of the top and bottom arms, and two poles located in the middle of the left and right arms of the square ring. If the excitation port is changed to *port 2*, we have the T_{010}^z mode and the field configuration is rotated by 90° (Hong, 1995). By adding a square patch as a perturbation at $\phi = 45^\circ$ these two degenerate modes are coupled and a dual-mode resonator can be obtained (Hong, 1995 and Curtis, 1991). The dimension of the square patch controls the coupling between the two degenerate modes (Chen, 2008).

The dimension of square patch perturbation is set to $d = 1.2$ mm to obtain optimal results. The feed line widths W_1 and W_2 are fixed to 0.2 mm and 0.576 mm respectively, to achieve acceptable insertion loss and matched to 50Ω line connectors. The feedlines length is $L_f = 14$ mm, and the gap size is $G = 0.1$ mm. The structure in Figure 3 is simulated using EM simulator software (EM, 2006) and the results are shown in Figure 4.

The simulation results exhibit that the specifications for narrowband filter at WiMax frequency is obtained. The minimum insertion loss is 1.5 dB and the return loss better than -25 dB. The fractional bandwidth is about 5.1%. The two transmission zeros are located at 2.1GHz, and 2.62GHz, having a sharp rejection of more than 40 dB.

4.1 Extracting External Quality Factor, Q_e

The external quality factors can be extracted by using EM simulator software (EM, 2006). This method of extracting external quality factor is illustrated in Figure 5, where the single-mode resonator is set as weakly coupled to its feed at one side. The dimensions of the resonator shown in Figure 2(a) are $a = 12.2$ mm, $W_1 = 0.2$ mm, $W_2 = W = 0.576$ mm, and $G = 0.1$ mm. By using the simulation results from the EM simulator (EM, 2006) shown in Figure 6, Q_e can be calculated by using (Hong, 2001):

$$Q_e = \frac{f_0}{BW_{3dB}} \quad (5)$$

Where f_0 is the center resonating frequency, and BW_{3dB} is the 3dB bandwidth, expressed as:

$$BW_{3dB} = f_2 - f_1 \quad (6)$$

Substituting $f_1 = 2.25$ GHz and $f_2 = 2.34$ GHz in Equation (6), the 3dB bandwidth, $BW_{3dB} = 0.09$ is achieved, then by replacing it and $f_0 = 2.3$ GHz in Equation (5), the $Q_e = 25.5$ is obtained.

4.2 Extracting the Coupling Coefficient

Since a dual-mode resonator operates as two resonators, coupling coefficient exists between them. Coupling coefficient between resonators can be extracted by using the EM simulator. In this method, the resonators should be weakly coupled to their feeds on both sides as depicted in Figure 7. The coupling coefficient is calculated using the simulation result shown in Figure 8 and the general formulation for extracting the coupling coefficient, k_{12} between the first and the second modes is expressed by Equation (7) (Hong, 2001):

$$k_{12} = \frac{f_2^2 - f_1^2}{f_2^2 + f_1^2} \quad (7)$$

Where f_1 and f_2 are the resonant frequencies of mode 1 and mode 2, respectively as illustrated in Figure 8.

For optimal design, with $d = 1.2$ mm, two degenerate modes frequencies obtained are shown in Figure 8. Substituting $f_1 = 2.27$ GHz, and $f_2 = 2.36$ GHz, in Equation (7), the coupling coefficient in this design is obtained $k_{12} = 0.0388$. Since the modes frequencies change by perturbation size therefore, the coupling coefficient is a function of the perturbation size (d). The variation of coupling coefficient, k_{12} versus perturbation size, d is demonstrated in Figure 9.

5. Experimental Results

The filter is fabricated using standard photolithography process on R/T Duroid 6010 having relative permittivity, $\epsilon_r = 10.2$, 0.636 mm of substrate thickness, and substrate loss of $\tan \delta = 0.0023$. Figure 10 shows the photograph of the BPF and its dimensions with respect to Figure 3 are shown in Table 1. As shown in Figure 10, two 50Ω SMA connectors are joined to 50Ω feedlines to connect to the Vector Network Analyzer (VNA) for measurement in the best matching condition. The measurement was performed using an HP8510B Vector Network Analyzer.

Figure 11 shows that the simulated and measured results are in good agreement. The fractional bandwidth is about 5.1%, the return loss is better than -20 dB and the minimum insertion loss of the filter is 1.68 dB. Conductor loss, and connector mismatches are the main factors to contribute to the total loss. By using superconductors and designing with

very narrow gap feedlines, using micromachining technique can reduce the insertion loss to its minimum, but it should be mentioned that the size of the coupling gaps between the feedlines and ring resonator affects not only the strength of coupling but also the resonant frequency (Chang, 1987 and Hsieh, 2003). Furthermore, micromachining is costly and superconductors need the use of cryostats that makes the application limited and not robust. In this design, some simple techniques are used to improve the filter performance. One of them is using proper substrate material with high dielectric constant and low loss tangent. This leads to having more compact size and lower insertion loss in passband. It is also possible to increase the system performance by using good feed line structure including proper feed line gap, width and length. Another simple technique used here in this filter design is the 45° mitered bend that helps to have less insertion loss and better return loss with simpler and cost effective fabrication, compared to similar designs reported in (Hong, 1995, Chen. C. H., 2007 and Hsieh, 2000). A research in (Razalli, 2008), presents four types of bending (discontinuity), and shows that 45° mitered bend technique gives the lowest insertion loss and the best return loss in passband.

6. Conclusions

A compact narrowband bandpass filter using dual-mode microstrip square loop resonator is designed and tested. The simulated and measured results are in good agreement. The dual-mode was excited by adding a square patch to the resonator, and a narrowband bandpass filter was introduced. In this design, the minimum measured insertion loss is 1.68 dB and the return loss better than -20 dB operating at 2.3GHz with a fractional bandwidth of 5.1% with two transmission zeros on both sides of the passband. It is fabricated on Duroid 6010 substrate having a relative dielectric constant of 10.2 and 0.635 mm of thickness. By applying proper substrate material, feedlines gap, length and width, as well as 45° mitered bend; the filter performance has been enhanced. This filter is attractive for further development and hence, it could be applied to support modern wireless communications and WiMax applications as it offers compactness in size with good performance and sharp rejection.

References

- Chang, K. (2004). *Microwave Ring Circuits and Related Structures*, New York: John Wiley & Sons.
- Chang. K., Martin. T. S., Wang. F., and Klein. J. L. (1987). On the Study of Microstrip Ring and Varactor-Tuned Circuits. *IEEE Transactions on Microwave Theory and Techniques*, Vol. 35, 1288-1295.
- Chen. C. H., Lin. Y. F., and Chen. H. M. (2007). Miniaturized Dual-Mode Bandpass Filter Using Mender Square Ring Resonator. *IEEE Conference on Electronic Devices and Solid State Circuits*, 777-780.
- Chen. Z. X., Dai. X. W., and Liang. C. H. (2007). Novel Dual-Mode Dual-Band Bandpass Filter Using Double Square-Loop Structure. *Progress In Electromagnetics Research*, PIER 77, 409-416.
- Curtis. J. A., and Fiedziuszko. S. J. (1991). Miniature dual mode microstrip filters. *IEEE MTT-S Digest*, Vol. 2, 443-446.
- El-Shaarawy. H. B., Coccetti. F., Plana. R., El Said. M., Hashish. E. A. (2008). Compact Bandpass Ring Resonator Filter with Enhanced Wide-Band Rejection Characteristics Using Defected Ground Structures. *IEEE Microwave and Wireless Components Letters*, Vol. 18, 500-502.
- EM. User's Manual, Computer Simulation Technology (CST) Microwave Studio, Version 2006B.
- Hong. J. S., Lancaster. M. J. (1995). Bandpass Characteristics of New Dual-Mode Microstrip Square Loop Resonators. *Electronics Letters*, Vol. 31, No. 11, 891-892.
- Hong, J. S., and Lancaster, M. J. (2001). *Microstrip Filters for RF/Microwave Applications*, New York: John Wiley & Sons.
- Hsieh. L. H., Chang. K. (2003). Compact, Low Insertion-Loss, Sharp-Rejection, and Wide-Band Microstrip Bandpass Filters. *IEEE Transactions on Microwave Theory and Techniques*, Vol. 51, No. 4, 1241-1246.
- Hsieh. L. H., Chang. K. (2000). Compact Dual-Mode Elliptic-Function Bandpass Filter Using a Single Ring Resonator with One Coupling Gap. *Electronic Letters*, No. 19, Vol. 36, 1626-1627.
- Pozar, D. M. (2005). *Microwave Engineering*, New Jersey: John Wiley & Sons.
- Razalli. M. S., Ismail. A., Mahdi. M. A., and Hamidon. M. N. (2008). Novel Compact Microstrip Ultra-Wideband Filter Utilizing Short-Circuited Stubs With Less Vias. *Progress In Electromagnetics Research*, PIER 88, 91-104.
- Wolff. I. and Knoppik. N. (1971). Microstrip Resonator and Dispersion Measurements on Microstrip Lines. *Electronics Letters*, Vol. 7, 779-781.

Table 1. Dimensions of “dual-mode filter”, with reference to the layout depicted in Figure 3

Parameter	Dimension (mm)
Perturbation size, d	1.2
Feedlines length, L_f	14
Feedgaps size, G	0.1
Feedlines width, W_1	0.2
Feedlines width, W_2	0.576
Resonator width, W	0.576
Side length of square resonator, a	12.2

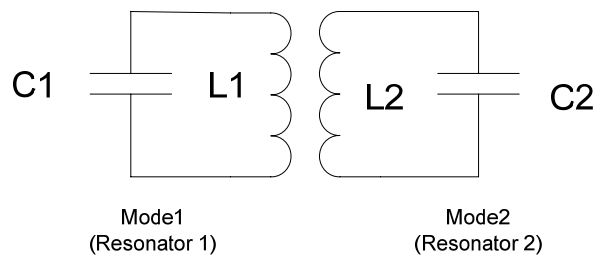


Figure 1. Lumped element equivalent circuit of a dual-mode resonator

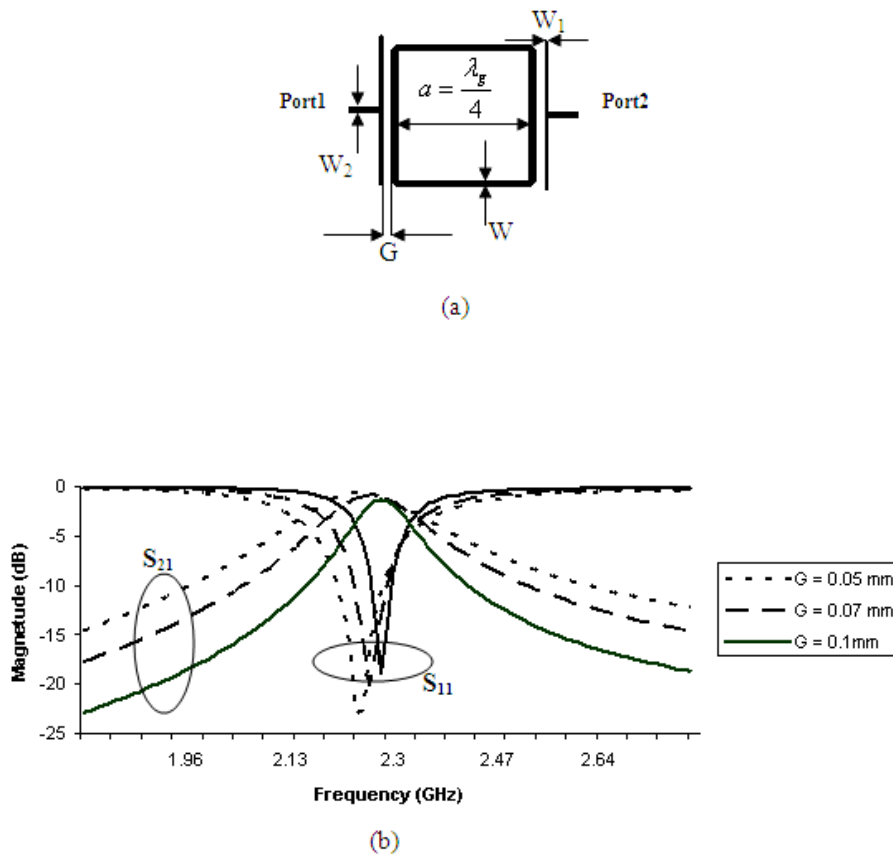


Figure 2. (a) Single mode square ring resonator, (b) simulation results (insertion loss, S_{21} and return loss, S_{11}) of a single mode resonator for different values of G .

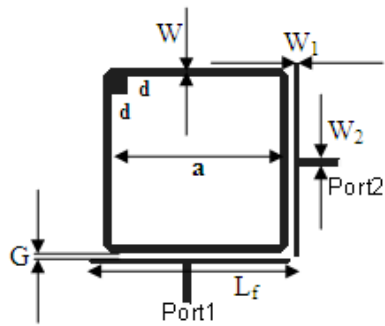


Figure 3. Dual-mode bandpass filter

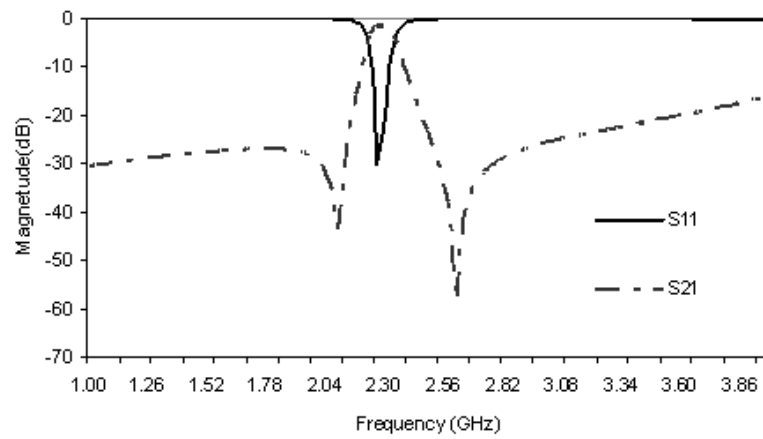


Figure 4. The simulation results for dual-mode filter

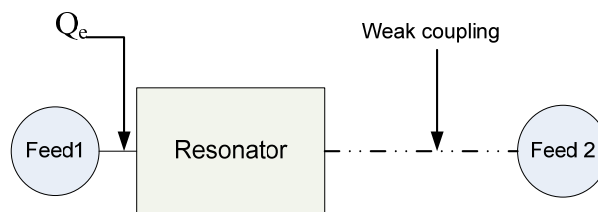


Figure 5. Extracting Q_e using EM simulator

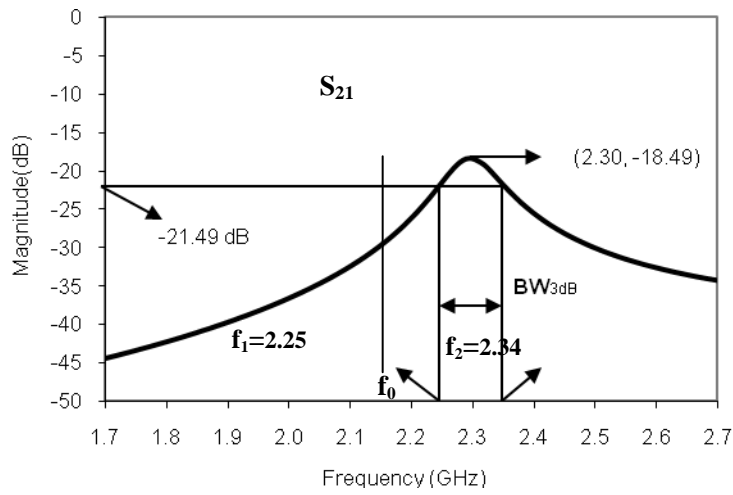


Figure 6. Simulated S_{21} for calculating Q_e .

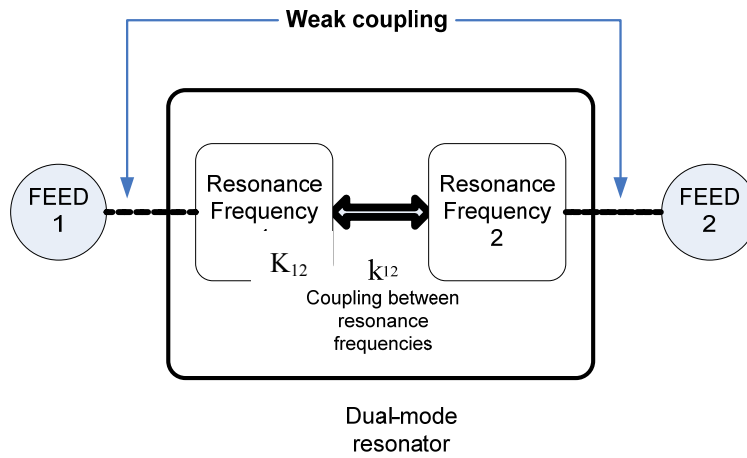


Figure 7. Extraction of coupling coefficient between resonators using an EM simulator

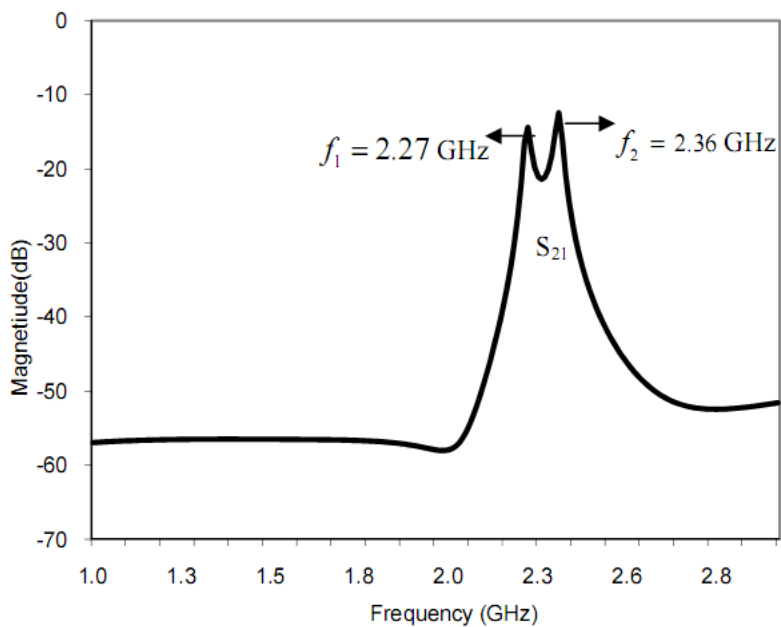


Figure 8. Simulated S_{21} for calculating coupling coefficient

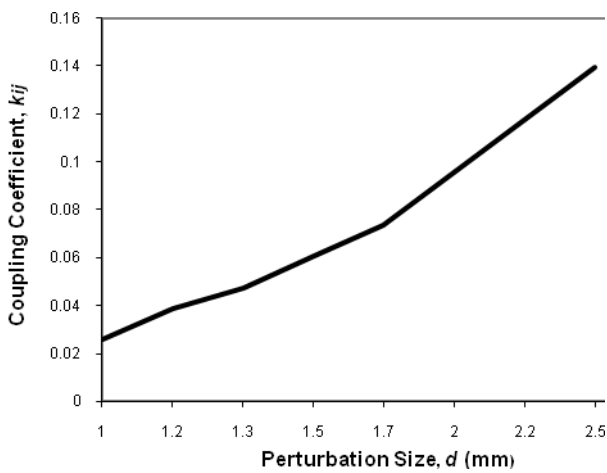


Figure 9. Variation of coupling coefficient, k_{ij} with perturbation size, d .

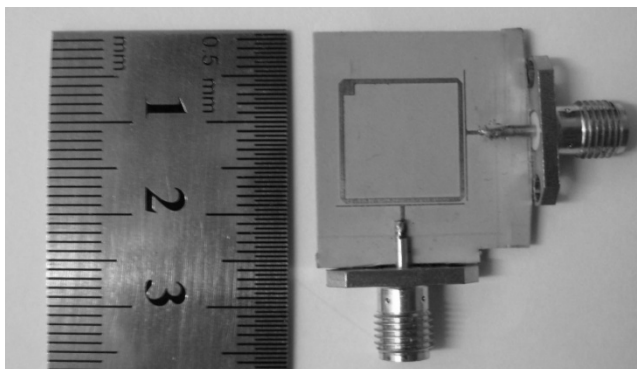
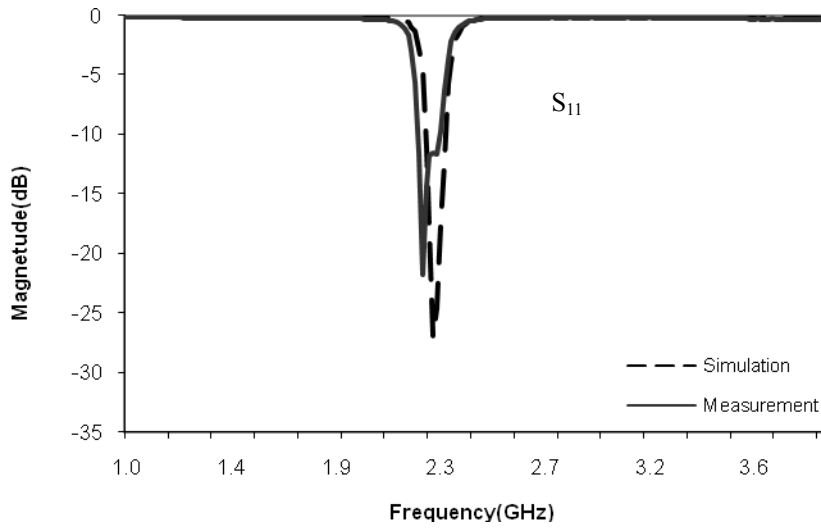
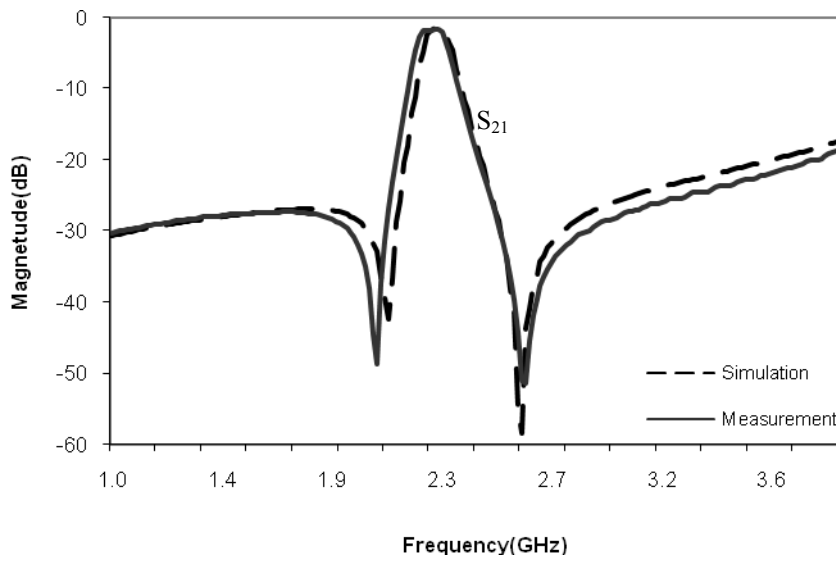


Figure 10. The photograph of the BPF



(a)



(b)

Figure 11. Measured and simulated results for the dual-mode filter
 (a) Return loss, S_{11} (b) Insertion loss, S_{21} .